Validation Experiments with the NCAR Spectral Element Dynamical Core

Richard D. Loft, Stephen J. Thomas
Scientific Computing Division
National Center for Atmospheric Research, Boulder, CO

Lorenzo M. Polvani, Richard K. Scott
Dept of Applied Physics and Applied Mathematics
Columbia University, New York, NY

1. Introduction

Traditionally, climate model dynamical cores have been based on the spectral transform method because the global spherical harmonic basis functions provide an isotropic representation on the sphere. It is trivial to implement semi-implicit time stepping schemes, as the spherical harmonics are eigenfunctions of the Laplacian on the sphere and the resulting Helmholtz problem is diagonalized in spectral space. Spectral elements maintain the accuracy and exponential convergence rate exhibited by the spectral transform method and have proven to be effective in geophysical fluid dynamics by Taylor et al. (1997) and Iskandarani et al. (1995). The explicit time step is limited by the Courant condition for gravity waves. For spectral elements, stability is determined by the eigenvalues of the discrete spatial operators. With quadratic clustering of Gauss points at element boundaries, these eigenvalues scale as $1/KN^2$, where K is the number of elements and N is the polynomial degree. For the spectral transform, the explicit time step decreases linearly with increased resolution. Consequently, the explicit time step is more restrictive in the case of spectral elements. A semi-implicit scheme removes the stability constraint related to gravity waves (Thomas et al 2003). The advection stability constraint can be avoided with a semi-Lagrangian scheme as described in Giraldo and Perot (2001).

In this article we perform validation experiments with a 3-D climate spectral element dynamical core developed at NCAR. The Held-Suarez (1994) idealized physical forcings are often used to evaluate numerical schemes for atmospheric general circulation models. We present results for this 1200 day integration using the spectral element model with explicit time-stepping and time-split diffusion. Results for a new benchmark proposed by Polvani et al (2002) are also reported. Initial conditions are specified without additional forcing terms. A major advantage of this test is that a 12 day integration is required.

2. Spectral Element Formulation of the Primitive Equations

The 3-D primitive equations neglect vertical acceleration and are derived from the Navier-Stokes equations by invoking scaling arguments for the atmospheric general circulation. We follow the NCAR CCM3 formulation described in Kiehl et al. (1996) and introduce a general, terrain-following, vertical coordinate η. This hybrid coordinate $\eta(\, p,\, p_s)$ is a monotonic function of pressure p and is dependent on the surface pressure p_s, where boundary conditions are given by $\eta(0, p_s) = 0$ and $\eta(p_s, p_s) = 1$. The momentum, thermodynamic and continuity equations for frictionless adiabatic motion are given by

$$\frac{D\mathbf{v}}{Dt} + f\,\mathbf{k}\times\mathbf{v} + \nabla\phi + R\,T\,\nabla\ln p = 0 \tag{2.1}$$

$$\frac{D\,T}{D\,t} - \frac{\kappa\,T\,\omega}{p} = 0 \tag{2.2}$$

$$\frac{\partial}{\partial\eta}\left(\frac{\partial p}{\partial t}\right) + \nabla\cdot\left(\mathbf{v}\,\frac{\partial p}{\partial\eta}\right) + \frac{\partial}{\partial\eta}\left(\dot\eta\,\frac{\partial p}{\partial\eta}\right) = 0 \tag{2.3}$$

where the material derivative is given by

$$\frac{D}{Dt} = \frac{\partial}{\partial t} + \mathbf{v}\cdot\nabla + \dot\eta\,\frac{\partial}{\partial\eta}$$

$\mathbf{v} = (\, u,\, v)$ is the horizontal velocity vector, T is the temperature R is the gas constant, c_p is the specific heat at constant pressure and $\kappa = R/c_p$. The geopotential ϕ is defined by the hydrostatic equation

$$\frac{\partial\phi}{\partial\eta} = -\frac{R\,T}{p}\,\frac{\partial p}{\partial\eta}, \tag{2.4}$$

and the vertical velocity $\omega \equiv Dp/Dt$ is given by

$$\omega = -\int_0^\eta \nabla\cdot\left(\mathbf{v}\,\frac{\partial p}{\partial\eta}\right)\,d\eta + \mathbf{v}\cdot\nabla p. \tag{2.5}$$

Expressions for log surface pressure $\ln p_s$ and vertical advection of pressure are obtained by integrating the continuity equation (2.3) using the boundary conditions $\dot\eta = 0$ at $\eta = 0$ and $\eta = 1$.

$$\frac{\partial}{\partial t}(\ln p_s) = -\frac{1}{p_s}\int_0^1 \nabla\cdot\left(\mathbf{v}\,\frac{\partial p}{\partial\eta}\right)\,d\eta \tag{2.6}$$

$$\dot\eta\,\frac{\partial p}{\partial\eta} = -\frac{\partial p}{\partial t} - \int_0^\eta \nabla\cdot\left(\mathbf{v}\,\frac{\partial p}{\partial\eta}\right)\,d\eta \tag{2.7}$$

The prognostic equations (2.1), (2.2), (2.6) for $\mathbf{v}$, T, and $\ln p_s$ are integrated using either an explicit or semi-implicit time-stepping scheme.

The hydrostatic relation (2.4) is used to diagnose the geopotential and the pressure p is obtained from the surface pressure p_s using the definition of the hybrid vertical coordinate. The vertical discretization employs finite differences and is designed to conserve both energy and angular momentum in the absence of external forcing terms. NLEV vertical layers are defined by the 'half-level' pressures $p_{l+1/2} = A_{l+1/2} + B_{l+1/2}\, p_s$. The constants $A_{l+1/2}$ and $B_{l+1/2}$ effectively define the vertical coordinate, where $B = \partial p / \partial p_s$. Prognostic variables are represented by 'full-level' values at pressure levels l. A hybrid terrain-following coordinate is a combination of sigma $\sigma = p/p_s$ and pure pressure levels. Pressure gradient truncation errors over steep topography can be significantly reduced by using η vertical coordinates (Simmons and Burridge 1981).

In the horizontal discretization via spectral elements, the computational domain Ω is partitioned into K elements Ω_k in which the dependent and independent variables are approximated by N–th order tensor-product polynomial expansions as described in Ronquist (1988). For example the velocity is expanded in terms of the N–th degree Lagrangian interpolants h_i,

$$\mathbf{u}_h^k(r_1, r_2) = \sum_{i=0}^{N} \sum_{j=0}^{N} \mathbf{u}_{ij}\, h_i(r_1)\, h_j(r_2)$$

A weak variational problem is obtained by integrating the equations with respect to test functions and directly evaluating inner products using Gauss-Lobatto quadrature.

$$(\, f,\, g\,)_{GL} \;=\; \sum_{k=1}^{K} \sum_{i=0}^{N} \sum_{j=0}^{N} f^k(\xi_i, \xi_j)\, g^k(\xi_i, \xi_j)\, \rho_i\, \rho_j$$

where $(\, \xi_i,\, \rho_i\,)$, $i = 0, \ldots N$ are the Gauss-Lobatto nodes and weights on $\Lambda = [\, -1,\, 1\,]$. Physical coordinates are mapped according to $\mathbf{x} \in \Omega_k \Rightarrow \mathbf{r} \in \Lambda \times \Lambda$. C^0 continuity of the velocity is enforced at inter-element boundaries which share Gauss-Lobatto points and direct stiffness summation is applied to assemble global matrices.

The primitive equations in general curvilinear coordinates are given in Loft et al. (2001). Following Sadourny (1972), a cubed-sphere coordinate system is employed whereby the sphere is tiled with rectangular elements by subdividing the six faces of the cube, which circumscribes the sphere, and then using a gnomonic projection to map these elements onto the surface of the sphere. Rancic et al (1996) showed that an equal angular projection results in a more uniformly spaced grid. Conformal coordinates for the cubed-sphere are discussed in this paper and by McGregor (1997). For a discussion on solving partial differential equations on the cubed-sphere, see the paper by Ronchi et al (1996).

3. Held-Suarez Results

The Held-Suarez (1994) (hereafter HS94) idealized climate test is designed to validate the dry dynamical core of an atmospheric general circulation model for multi-year integrations. It assumes an ideal gas atmosphere over a rotating sphere with no topography. The flow is not specified as hydrostatic, however, the hydrostatic primitive equations may be employed as described in Section 2. The prescribed forcing consists of a simple Newtonian relaxation of the temperature field to a zonally symmetric state and Rayleigh damping of the lower level wind field to approximate friction or drag caused by the atmospheric boundary layer near the surface. The initial state of the atmosphere is hydrostatic and isothermal $T = 300$ K. The model is integrated for 1200 days. Zonally averaged wind and temperature fields are then reported. The Held-Suarez forcings take the following form,

$$\frac{\partial \mathbf{v}}{\partial t} = \cdots - k_{\mathbf{v}}(\,\phi,\,\sigma\,)$$

$$\frac{\partial T}{\partial t} = \cdots - k_T(\,\phi,\,\sigma\,)\;[\,T - T_{\mathrm{eq}}(\,\phi,\,\sigma\,)\,]$$

where ϕ is the latitude and $\sigma = p/p_s$ is the vertical sigma coordinate level. The temperature is relaxed to the equilibrium temperature T_{eq} and relaxation rate k_T. The linear damping rate of the wind is given by $k_{\mathbf{v}}$. A simulation was performed using 150 spectral elements and 20 equally spaced sigma levels in the vertical direction. An explicit time step of $dt = 100$s was specified. A Boyd-Vandeven filter (Boyd 1996) was applied every second time step to stabilize the model. In addition, a ∇^2 dissipation with coefficient $\nu = 1 \times 10^4$ m^{2}s^{-1} was applied using an explicit time-splitting scheme, as described in Williamson and Laprise (2000). This implies that the dissipation term is integrated to first order.

The simulation results are plotted in Figures 1 and 2. These plots closely match those given in HS94 and exhibit the characteristic formation of jets in the upper atmosphere. We observe a slightly increased damping near the surface, in both the zonal temperature and zonal wind plots, where the amplitude of the wind shear near the equator is lower than that reported in the HS94 paper. In our experiments, we also observed that the placement of the jets is sensitive to the amount of dissipation. Values of ν larger than $\nu = 1 \times 10^5$ tend to cause the two jets to merge by moving inward towards the equator. This damping is less pronounced when the model is run without dissipation. However, dissipation is required for our second dynamical core test problem.

4. Baroclinic Instability

A clear limitation of the HS94 test case is the temporal and spatial averaging of the flow fields, which could possibly mask errors in the numerics. Another drawback is that analytically specified forcing terms must be applied and thus the dynamical core is not tested in isolation. Numerical convergence was not addressed by the authors, however, the issue was considered by Boer and Denis (1997). The test problem proposed by Polvani et al. (2002) is designed to overcome these limitations by specifying an initial boundary value problem (IBVP) for the primitive equations, including viscosity. A numerically converged solution should be obtained by any primitive equations dynamical core, simply by increasing the horizontal resolution.

The analytic initial condition specified in Polvani et al (2002) consists of a basic zonal flow, representing a mid-latitude tropospheric jet. A small perturbation is added to induce a baroclinic instability, which is then integrated for 12 days. The solution of the resulting IBVP is guaranteed to blow-up in a finite time unless dissipation terms are included in the momentum and thermodynamic equations. For the spectral element model, it is difficult to implement a $\nu\nabla^4$ hyper-viscosity and thus we consider the standard $\nu\nabla^2$ dissipation operator. The vertical discretization employs 20 equally spaced sigma levels, with the initial surface pressure set to $p_s = 1000$ hPa. Due to the zonal structure of the wind field and numerical integration in the meridional direction to compute the temperature field, the initial condition is first computed on a 1024×512 Gaussian lat-lon grid corresponding to a T341 spectral resolution. The initial fields are then computed on the cubed-sphere spectral element mesh using bilinear interpolation on each vertical level.

The explicit spectral element dynamical core was integrated for twelve days using time-split dissipation with viscosity coefficient $\nu = 5 \times 10^5$ m^{2}s^{-1}, as specified by the authors. A horizontal resolution roughly equivalent to a spectral transform model with a triangular truncation of T170 was employed. The temperature field at the surface ($\sigma = 0.975$) after 10 days of integration is plotted in Figure 3. The onset of the baroclinic instability and the resulting nonlinear wave-breaking are clearly visible in this plot. The eddy kinetic energy (EKE) computed after 10 days is 1.7×10^4 Jm^{-2}. The surface vorticity at 10 days is plotted in Figure 4 and diagnostic quantities such as $\|\zeta\|_2$ and $\|\zeta\|_\infty$ are in agreement with those reported in Polvani et al (2002). These results also compare closely with the GFDL FMS-SDC spectral transform model, as reported in this paper. Indeed, it is our conclusion that the NCAR spectral element model has very nearly converged to the same solution.

References

Boer, G. J., and B. Denis, 1997: Numerical convergence of the dynamics of a GCM. *Climate Dynamics*, **13**, 359–374.

Boyd, J. P., 1996: The erfc-log filter and the asymptotics of the Euler and Vandeven sequence accelerations. *Proceeding of the Third International Conference on Spectral and High Order Methods*. eds. A. V. Ilin and L. Ridgway Scott. Houston Journal of Mathematics. 267–276.

Giraldo, F. X. and J. B. Perot, 2001: A spectral element Semi-Lagrangian (SESL) method for the spherical shallow water equations . *J. Comp. Phys*, submitted.

Held, I. H., and M. J. Suarez, 1994: A proposal for the intercomparison of the dynamical cores of atmospheric general circulation models. *Bull. Amer. Met. Soc.*, **75**, 1825–1830.

Kiehl, J. T., J. J. Hack, G. B. Bonan, B. A. Boville, B. P. Briegleb, D. L. Williamson, P. J. Rasch, 1996: Description of the NCAR community climate model (CCM3). NCAR Technical Note, NCAR/TN-420+STR.

Loft, R. D., S. J. Thomas, and J. M. Dennis, 2001: Terascale spectral element dynamical core for atmospheric general circulation models. Proceedings of ACM/IEEE Supercomputing 2001.

McGregor, J. L., 1997: Semi-Lagrangian advection on a cubic gnomic projection of the sphere. *Numerical Methods in Atmospheric and Oceanic Modeling*. The Andre J. Robert Memorial Volume, CMOS and NSERC Research Press, 1997. pages 153-169.

Polvani, L. M., R. K. Scott, and S. J. Thomas, 2002: An initial-value problem for testing the dynamical core of atmospheric general circulation models. *Mon. Wea. Rev.*, submitted.

Rancic, M., R. J. Purser, and F. Mesinger, 1996: A global shallow-water model using an expanded spherical cube: Gnomic versus conformal coordinates. *Q. J. R. Meteorol. Soc.*, **122**, 959–982.

Ronquist, E. M., 1988: *Optimal Spectral Element Methods for the Unsteady Three Dimensional Navier Stokes Equations*, Ph.D Thesis, Massachusetts Institute of Technology, 176p.

Sadourny, R., 1972: Conservative finite-difference approximations of the primitive equations on quasi-uniform spherical grids. *Mon. Wea. Rev.*, **100**, 136–144.

Ronchi, C., R. Iacono and P. S. Paolucci, 1996: The "cubed sphere": A new method for the solution of partial differential equations in spherical geometry. *J. Comp. Phys.*, **124**, 93-114.

Simmons, A. J. and D. M. Burridge, 1981: An energy and angular-momentum conserving finite-difference scheme and hybrid vertical coordinates. *Mon. Wea. Rev*, **109**, 758–766.

Taylor, M., J. Tribbia, and M. Iskandarani, 1997: The spectral element method for the shallow water equations on the sphere. *J. Comp. Phys.*, **130**, 92–108.

Thomas, S. J., J. M. Dennis, H. M. Tufo, and P. F. Fischer, 2003: A Schwarz preconditioner for the cubed-sphere. *SIAM J. Sci. Comp.*, to appear.

Williamson, D. L., and R. Laprise, 2000: Numerical approximations for global atmospheric GCMs. *Numerical modeling of the global atmosphere in the climate system*, eds P. Mote and A. O'Neill. Proc. NATO Adv. Stud. Inst., 1998. 127–219, Kluwer Acad. Publ., 517 pp.

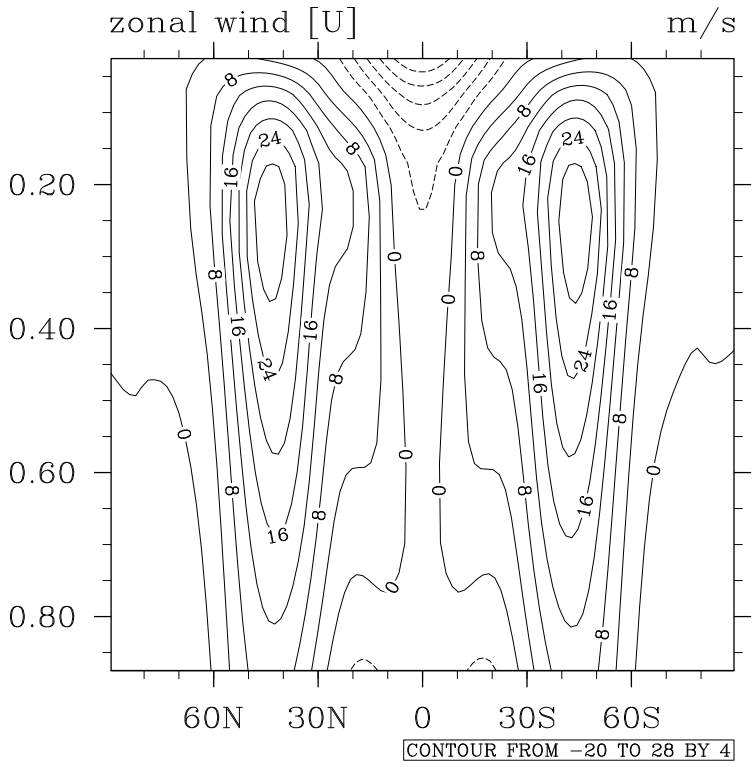

Figure 1: Held-Suarez idealized forcings. Zonal-mean wind. 1000 day mean. Integration with $\nu\nabla^2$ time-split explicit diffusion, $\nu = 1\times10^4$ m^{2}s^{-1}. Boyd-Vandeven Filter, $\mu = 0.10$, $f = 2$. Results from explicit SEAM, $ne = 5$, $nv = 8$.

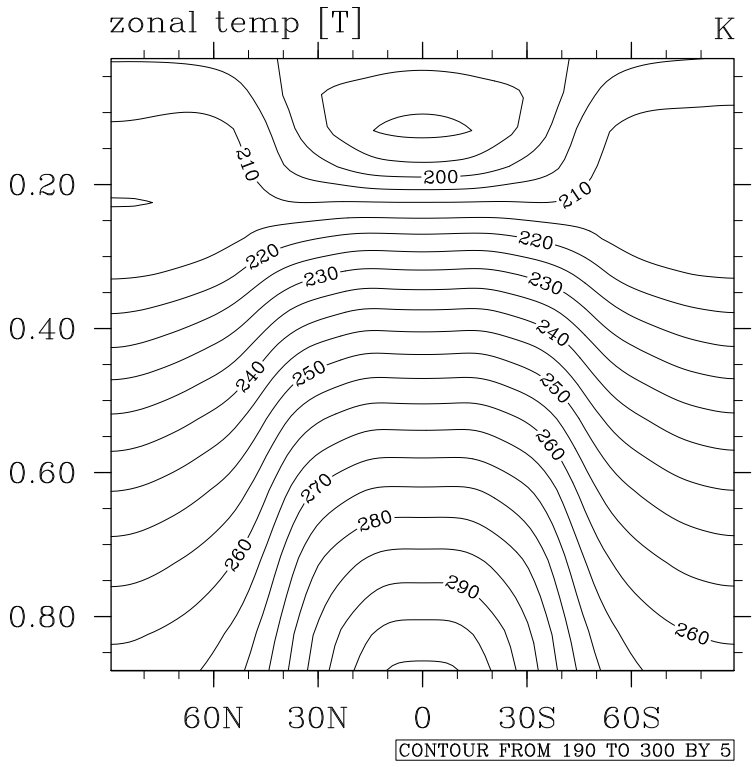

Figure 2: Held-Suarez idealized forcings. Zonal-mean temperature. 1000 day mean. Integration with $\nu\nabla^2$ time-split explicit diffusion, $\nu = 1 \times 10^4$ m^{2}s^{-1}. Boyd-Vandeven Filter, $\mu = 0.10$, $f = 2$. Results from explicit SEAM, $ne = 5$, $nv = 8$.

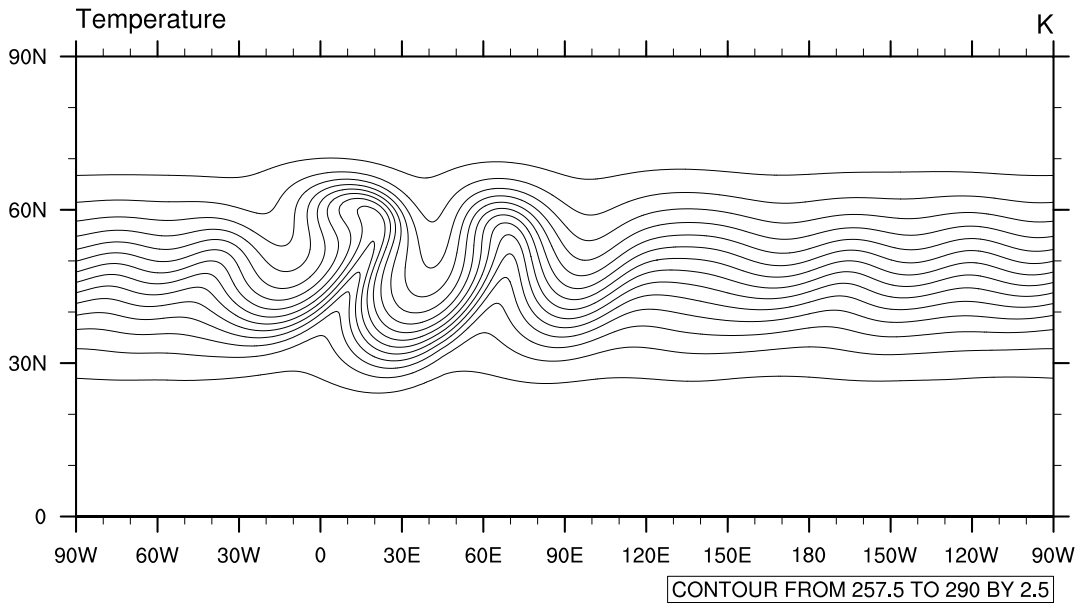

Figure 3: Surface temperature (at $\sigma = 0.975$) after 10 days of integration with $\nu\nabla^2$ time-split explicit diffusion, $\nu = 5 \times 10^5$ m^{2}s^{-1}. Results from explicit SEAM, $ne = 21$, $nv = 8$, C147L20 (T170 equivalent) resolution.

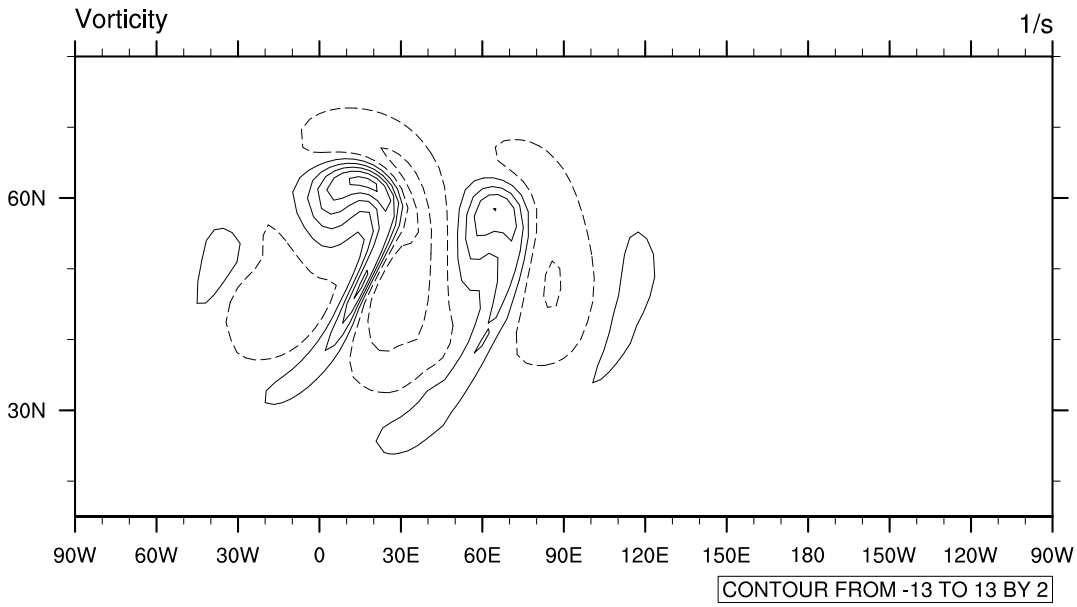

Figure 4: Surface vorticity (at $\sigma = 0.975$) after 10 days of integration with $\nu\nabla^2$ time-split explicit diffusion, $\nu = 5.0 \times 10^5$ m^{2}s^{-1}. Results from explicit SEAM, $ne = 21$, $nv = 8$, C147L20 (T170 equivalent) resolution.